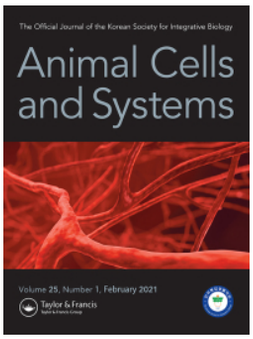

Animal Cells and Systems

ISSN: (Print) (Online) Journal homepage: www.tandfonline.com/journals/tacs20

Lamin A/C facilitates DNA damage response by modulating ATM signaling and homologous recombination pathways

Seong-jung Kim, Su Hyung Park, Kyungjae Myung & Kyoo-young Lee

To cite this article: Seong-jung Kim, Su Hyung Park, Kyungjae Myung & Kyoo-young Lee (2024) Lamin A/C facilitates DNA damage response by modulating ATM signaling and homologous recombination pathways, Animal Cells and Systems, 28:1, 401-416, DOI: 10.1080/19768354.2024.2393820

To link to this article: https://doi.org/10.1080/19768354.2024.2393820

Published online: 20 Aug 2024.

ANIMAL CELLS AND SYSTEMS
2024, VOL. 28, NO. 1, 401–416
https://doi.org/10.1080/19768354.2024.2393820

Lamin A/C facilitates DNA damage response by modulating ATM signaling and homologous recombination pathways

Seong-jung Kim[a,b]#, Su Hyung Park[a,c]#, Kyungjae Myung[a,c] and Kyoo-young Lee[a,d]

[a]Center for Genomic Integrity, Institute for Basic Science, Ulsan, Korea; [b]Department of Biological Sciences, College of Information-Bio Convergence Engineering, Ulsan National Institute of Science and Technology, Ulsan, Korea; [c]Department of Biomedical Engineering, College of Information-Bio Convergence Engineering, Ulsan National Institute of Science and Technology, Ulsan, Korea; [d]Department of Biochemistry, College of Medicine, Hallym University, Chuncheon, Korea

ABSTRACT

Lamin A/C, a core component of the nuclear lamina, forms a mesh-like structure beneath the inner nuclear membrane. While its structural role is well-studied, its involvement in DNA metabolism remains unclear. We conducted sequential protein fractionation to determine the subcellular localization of early DNA damage response (DDR) proteins. Our findings indicate that most DDR proteins, including ATM and the MRE11-RAD50-NBS1 (MRN) complex, are present in the nuclease – and high salt-resistant pellet fraction. Notably, ATM and MRN remain stably associated with these structures throughout the cell cycle, independent of ionizing radiation (IR)-induced DNA damage. Although Lamin A/C interacts with ATM and MRN, its depletion does not disrupt their association with nuclease-resistant structures. However, it impairs the IR-enhanced association of ATM with the nuclear matrix and ATM-mediated DDR signaling, as well as the interaction between ATM and MRN. This disruption impedes the recruitment of MRE11 to damaged DNA and the association of damaged DNA with the nuclear matrix. Additionally, Lamin A/C depletion results in reduced protein levels of CtIP and RAD51, which is mediated by transcriptional regulation. This, in turn, impairs the efficiency of homologous recombination (HR). Our findings indicate that Lamin A/C plays a pivotal role in DNA damage repair (DDR) by orchestrating ATM-mediated signaling, maintaining HR protein levels, and ensuring efficient DNA repair processes.

ARTICLE HISTORY
Received 9 July 2024
Revised 5 August 2024
Accepted 11 August 2024

KEYWORDS
DNA damage response (DDR); Lamin A/C; ATM; MRN complex

Introduction

DNA double-strand breaks (DSBs) represent one of the most deleterious genomic lesions and improper DSB repair can lead to genomic instability. DSBs are detected by sensor proteins, which initiate the DNA damage response (DDR), a multi-step signal transduction pathway (Shiloh 2006). Ataxia-telangiectasia mutated (ATM), a serine-threonine kinase, is a primary DSB sensor. Upon detection of a DSB, ATM is autophosphorylated at serine 1981 (S1981), thereby activating itself (Bakkenist and Kastan 2003). Upon activation, ATM phosphorylates a number of DDR proteins, including H2AX, MRE11, RAD50, NBS1, BRCA1, and CHK2 (Rogakou et al. 1998, Savic et al. 2009, Shiloh 2014, Lavin et al. 2015). Phosphorylation of H2AX at serine 139 (γH2AX) recruits the MRE11/RAD50/NBS1 (MRN) complex and MDC1 to the DNA damage site (Stucki et al. 2005, Lavin et al. 2015). This process enhances further MRN recruitment and subsequent ATM activation, creating a positive feedback loop for proper DDR signaling (D'Amours and Jackson 2002, Lee and Paull 2005, Dupre et al. 2006).

The activation of ATM-mediated DDR signals results in the arrest of the cell cycle and the subsequent activation of DSB repair (DSBR) pathways (Groelly et al. 2023). The phosphorylation of NBS1 by ATM is essential for the phosphorylation of a checkpoint protein, CHK2, and SMC1. RAD50 is phosphorylated by ATM and ATR, another key DDR kinase, which facilitates the phosphorylation of another checkpoint protein, CHK1. Cells utilize distinct DSBR pathways, including homologous recombination (HR) and non-homologous end-joining (NHEJ), contingent upon their respective cell cycle phase and the availability of a sister chromatid as a repair template (Shibata 2017). MDC1 recruitment to DNA damage sites results in RNF8 and RNF168 recruitment, which in turn catalyzes protein ubiquitination at

CONTACT Kyoo-young Lee kylee@hallym.ac.kr Department of Biochemistry, College of Medicine, Hallym University, Chuncheon 24252, Korea
#These authors contributed equally to this work.
This article has been corrected with minor changes. These changes do not impact the academic content of the article.

DSB sites and attracts resection enzymes such as EXO1, DNA2, and CtIP, thus facilitating efficient HR processes (Fontana et al. 2018). Furthermore, it was reported that phosphorylation of MRE11 by ATM is essential for HR, as it facilitates RAD51 foci formation and EXO1 phosphorylation (Kijas et al. 2015).

The nuclear lamins are intermediate filaments that constitute the nuclear lamina, a meshwork structure located underneath the nuclear envelope (Aebi et al. 1986). Mammalian cells contain two major lamins (Shimi et al. 2008, Gesson et al. 2016). A-type lamins are encoded by the *LMNA* gene, which undergoes alternative splicing to yield Lamin A and Lamin C. B-type lamins are encoded by two genes *LMNB1* and *LMNB2*. Previous researches suggest the involvement of Lamin A/C in DNA replication, as disrupting lamin organization in the Xenopus laevis nucleus inhibits replication (Spann et al. 1997, Moir et al. 2000). A related study has recently reported the presence of replication factor complex C (RFC) and RFC-like complex proteins in the nuclease – and high salt-resistant protein fractions. (Lee and Park 2020, Park et al. 2021).

In addition to the discovery of the role of the nuclear lamina as a tether of chromosomes via lamina-associated domains (Guelen et al. 2008, Kind et al. 2013, Kind and van Steensel 2014, van Steensel and Belmont 2017), the presence of a nucleoplasmic pool of Lamin A/C has prompted further questions about its involvement in DNA replication as well as DNA damage repair (Bridger et al. 1993, Moir et al. 2000). Some studies have suggested that damaged DNA is tethered to the nuclear structure in order to be efficiently repaired (McCready and Cook 1984, Harless and Hewitt 1987, Koehler and Hanawalt 1996). Furthermore, the preferential repair of nuclear matrix-associated DNA has been reported. Accordingly, Lamin A/C maintains the positional stability of DNA damage repair sites (Mahen et al. 2013). Additionally, there have been reports on the nuclear matrix association of DDR and DSBR proteins, including BRCA1, BRCA2, and RAD51 (Qiao et al. 2001, Mladenov et al. 2006, Xia et al. 2006, Kubota et al. 2009). Some studies on Lamin A/C have uncovered its role in HR by regulating the transcription of 53BP1, RAD51, and BRCA1 (Gonzalez-Suarez et al. 2009, Redwood et al. 2011, Redwood et al. 2011, Mayca Pozo et al. 2017, Li et al. 2018). Moreover, another study demonstrated that Lamin A/C interacts with a DDR protein, 53BP1, to maintain its protein stability (Gonzalez-Suarez et al. 2009, Gibbs-Seymour et al. 2015). Lamin A/C also facilitates the accumulation of 53BP1 at damage sites, the positional stability of DNA damage repair foci, and efficient HR following ionizing radiation (IR) treatment (Redwood et al. 2011). However, the detailed mechanisms of how the nuclear matrix structure and Lamin A/C are involved in the different steps of DNA repair processes remain poorly understood.

Here, we uncovered the critical role of Lamin A/C in orchestrating the damaged DNA and DDR/HR proteins. Utilizing a stepwise protein fractionation method, we discovered that the ATM and MRN complex proteins are found in nuclease-resistant protein fractions. This fractionation profile was maintained throughout the cell cycle or IR-induced DNA damage. Instead, Lamin A/C directly interacts with ATM and MRN proteins, but may not be required for their association with the nuclear matrix. Rather, Lamin A/C regulates DDR protein recruitment and DDR signaling by allowing stable interaction between ATM and MRN complex. Furthermore, Lamin A/C regulates HR efficiency by maintaining the levels of HR proteins.

Materials and methods

Cell lines and cell culture

Human embryonic kidney (HEK) 293 T, Osteosarcoma epithelial cells (U2OS), HeLa cells, and U2OS 2-6-5 cells stably expressing destabilization domain (DD)-estrogen receptor (ER)-FokI endonuclease-mCherry-Lac repressor (LacR) fusion protein (DD-ER-FokI-mCherry-LacR) (kindly provided by Dr. Roger Greenberg) were culture in Dulbecco's modified Eagle's medium supplemented with 10% fetal bovine serum (GE Healthcare), 100 U/mL penicillin G (Life Technologies), and 100 µg/mL streptomycin (Life Technologies) in a humidified atmosphere of 5% CO_2 at 37°C.

Reagents and antibodies

The following drugs were used in this study: MG-132, cyclohexamide, RO-3306, thymidine (Sigma-Aldrich). The following antibodies were used in this study: anti-phospho ATM (S1981) antibodies (R&D Systems, Inc.), anti-NBS1, anti-MRE11 antibodies (Novus Biologicals), anti-RAD50 antibody (GeneTex), anti-RNF8, anti-PARP1, anti-BRCA2, anti-53BP1, anti-MDC1 antibodies (Abcam), anti-CtIP antibody (Active Motif, Inc.), anti-CHK1, anti-CHK2, anti-phospho CHK1 (S345), anti-phospho CHK2 (T68), anti-phospho P53 (S15), anti-RAD51, anti-phospho NBS1 (S343) antibodies (Cell signaling Tech), anti-ATM, anti-Lamin A/C antibodies (Bethyl Laboratories), anti-GFP, anti-P53, anti-RIF1, anti-Lamin B1 antibodies (Santa Cruz Biotechnology), anti-Ku80, anti-Histone H3 antibodies (Thermo Fisher Scientifics), anti-phospho H2AX (S139), anti-BRCA1 antibodies (MERCK millipore), anti-α-tubulin, anti-FLAG antibodies (Sigma-Aldrich).

Plasmids, small interfering RNAs (siRNAs), and transfection

GFP-tagged Lamin cDNAs were kindly provided by Dr. Bum-Joon Park (Lee et al. 2016). Mre11 cDNA was cloned into pcDNA3.1(+) containing MYC-tag. CtIP cDNA was cloned into pEGFP-N1. Flag-tagged ATM plasmid was purchased from Addgene (31985). The following synthetic duplex siRNAs were purchased: *LMNA* (#SN-4001-1), *CtIP* (#SN-5932-1), *LIG4* (#SN-3981), and control siRNA (#SN-1002) (Bioneer). *RAD51* siRNA was purchased from Thermo Fiher Scientific (#130717). Transfection of plasmid DNA and small interfering RNAs (siRNA, 20nM) were performed using Transporter 5 reagent (Polysciences Inc) and RNAiMAX (Thermo Fisher Scientific), respectively, according to the manufacturer's instructions. Transfection reagents were removed 6 h post-transfection, and fresh medium was added. Cells were analyzed at 48 h after transfection.

Cell cycle synchronization and analysis

To obtain cells at G1 and S phase, cells were first arrested at the G2 phase by treatment with 10 μM CDK1 inhibitor (RO-3306) for 16 h. Cells were then washed and incubated in fresh media containing 2 mM thymidine for 17 h to arrest at the G1/S boundary. Cells were then released into fresh media for 3 h (S), 8 h (G2/M) and 13 h (G1). The cell cycle was identified based on DNA content assessed by propidium iodide staining. Data analysis was performed using FlowJo software.

Subcellular fractionation

Subcellular fractionation was performed as described by (He et al. 1990) with slight modifications. Five million HEK-293 T cells were incubated in 200 μL CSK buffer (10 mM PIPES, 100 mM NaCl, 300 mM sucrose, 2 mM $MgCl_2$, 1 mM EGTA, and 0.5% Triton X-100) for 5 min at 4°C, followed by centrifugation. The supernatant was collected as the 'soluble fraction', while the pellet was washed in CSK buffer and then lysed with 70 μL CSK buffer supplemented with Benzonase® nuclease (250 U/mL) and 5 mM $MgCl_2$ for 20 min at 37°C. A final concentration of 0.25 M ammonium sulfate was then added for 5 min at 4°C, followed by centrifugation to obtain the 'chromatin fraction'. The remaining nuclease-resistant pellet was washed with high salt CSK buffer (CSK buffer containing 2 M NaCl) for 5 min at 4°C, followed by centrifugation. The remaining nuclease-resistant and high-salt 'pellet fraction' was solubilized in 50 μL UB buffer (8 M urea, 10 mM NaCl, 5 mM $MgCl_2$, 250 mM sucrose, 1 mM EGTA, 10 mM Tris-HCl, pH 7.6) as described by (Mladenov et al. 2006)

Whole-cell extracts preparation

Whole-cell extracts were prepared by lysing cell pellets with RIPA buffer (50 mM Tris-HCl pH 8.0, 150 mM NaCl, 5 mM EDTA, 1% Triton X-100, 0.1% sodium dodecyl sulfate, 0.5% sodium deoxycholate) supplemented with 0.1 M phenylmethylsulfonyl fluoride, PhosSTOP Phosphatase Inhibitors, cOmplete Protease Inhibitors (Roche), and Benzonase® nuclease. The mixture was incubated on ice for 40 min, followed by sonication and centrifugation.

Immunoprecipitation and immunoblot analysis

For immunoprecipitation, cells were lysed in ice-cold buffer X (100 mM Tris-HCl, 250 mM NaCl, 1 mM EDTA, 1% NP-40) supplemented with 0.1 M phenylmethylsulfonyl fluoride, PhosSTOP phosphatase inhibitor cocktail (Roche), cOmplete protease inhibitor cocktail (Roche), and Benzonase® nuclease for 45 min, followed by sonication and centrifugation. Target proteins in the lysate were immunoprecipitated with the specified antibodies. For immunoblot analysis, proteins were separated by SDS-PAGE and transferred to a nitrocellulose membrane. Membranes were blocked in Tris-buffered saline containing 0.1% Tween 20 and 5% nonfat dry milk for 30 min and incubated with primary antibodies overnight. After washing, the blots were incubated with horseradish peroxidase-conjugated secondary antibodies (Enzo Life Sciences). Signals were detected using an enhanced chemiluminescence reagent (Thermo Fisher Scientific) and an automated imaging system (ChemiDoc MP, Bio-Rad Laboratories).

355-nm UV laser microirradiation, immunostaining, and image acquisition

For UV laser microirradiation, U2OS or HeLa cells were plated on LabTek™ Chambered Coverglasses (Thermo Fisher Scientific) and pre-sensitized with 10 μM BrdU for 24 h. UV microirradiation was applied using a 355-nm diode laser (100% power) projected through a C-Apochromat 40×/1.2W Korr FCS M27 objective through a bleaching module (7 iterations) of an LSM880 confocal microscope (Carl Zeiss, Oberkochen, Germany). Live cell images were acquired after irradiation with a time-lapse setting using ZEN 2.6 (blue edition) software (Carl Zeiss). GFP signal intensity on the microirradiated strip was quantified using ZEN 2.6 software. Relative intensities, adjusted to a baseline of 100, were displayed. For staining, cells on the slide were fractionated as previously

described and fixed with 4% paraformaldehyde. After washing with PBS and incubation in blocking buffer (10% FBS in PBS) for 30 min, cells were incubated with primary antibodies diluted in blocking buffer overnight at 4°C. After three washes with 0.05% Triton X-100 in PBS, Alexa Fluor-conjugated secondary antibodies (Thermo Fisher Scientific) were added and incubated for 30 min. After washing, cells were mounted with ProLong® Gold antifade reagent (Vector Laboratories, Burlingame, CA, USA). Confocal images were captured using an LSM880 confocal microscope (Carl Zeiss) with a 40×/1.2 objective. Image acquisition and analysis were performed using ZEN 2.6 (blue edition) software (Carl Zeiss).

X-ray irradiation

Cells were irradiated using RS 2000 X-ray irradiator (RAD SOURCE) according to the manufacturer's protocol.

FokI-induced DSB generation

U2OS-LacO reporter cells stably expressing DD-ER-FokI-mCherry-LacR were transfected with either siRNA or cDNA. After 48 h, the cells were treated with 1 μM tamoxifen (which binds to the ER and induces nuclear export of ER-fused proteins) and 1 μM Shield1 (which stabilizes DD domain-tagged proteins) for 5 h to induce DSBs. Cells were then fractionated and fixed for immunostaining.

I-SceI endonuclease-induced HR/NHEJ assay

An I-SceI-induced DSBR assay was performed using U2OS-based reporter cell lines (DR-GFP for HR and EJ5-GFP for NHEJ), according to the method described previously (Gunn and Stark 2012). Briefly, reporter cells were plated in a 12-well plate at a density of 1×10^5 cells per well. The next day, each cell line was transfected with 20 nM siRNA. After 24 h, the cells were retransfected with 0.5 μg of either pCAGGS-I-SceI or the empty pCAGGS-BSKX vector together with 0.1 μg of a dsRed expression vector. Two days after transfection with I-SceI, cells were analyzed using a Becton Dickinson FACSVerse flow cytometer with BD FACSuite software. Repair efficiency was determined by dividing the percentage of GFP-positive cells by the percentage of dsRed-positive cells. Data analysis was performed using FlowJo software, and experiments were repeated at least three times.

Reverse transcription quantitative PCR (RT-qPCR)

Total RNA was extracted using a TRIzol® Reagent (Thermo Fisher Scientific) protocol. RNA (3 μg) was used to synthesize cDNA using the SuperScript® IV First-Strand Synthesis System (Thermo Fisher Scientific) according to the manufacturer's instructions. RT-qPCR was performed using SYBR Green Master Mix (Applied Biosystems, Foster City, CA, USA) in a QuantStudio 7 Flex system (Applied Biosystems) according to the manufacturer's instructions. Gene expression was normalized with GAPDH expression. The following primers were used: *MRE11*-forward (For) (5′-AACGGGAACGTCTGGGTAAT-3′), *MRE11*-reverse (Rev) (5′-GGCTAAAGCGAAGAACACTGAA-3′), *RAD51*-For (5′-TCTCTGGCAGTGATGTCCTGGA-3′), *RAD51*-Rev (5′-TAAAGGGCGGTGGCACTGTCTA-3′), *MDC1*-For (5′-AGCAACCCCAGTTGTCATTC-3′), *MDC1*-Rev (5′-AGCGCTGCTGAGACTTCTTC-3′), *CtIP*-For (5′-CAGGAACGAATCTTAGATGCACA-3′), *CtIP*-Rev (5′-GCCTGCTCTTAACCGATCTTCT-3′), *P53*-For (5′-GTGTGGAATCAACCCACAGCTGCAC-3′), *P53*-Rev (5′-CCTGTCATCTTCTGTCCCTTCCCAG-3′), *LMNA*-For and Rev (P201515 V).

RPA retention assay using flow cytometry

IR-induced chromatin RPA2 was measured using a slightly modified protocol based on (Shibata et al. 2011). Cells were irradiated with X-ray and incubated for 2 h, and 4 μM aphidicolin (Sigma-Aldrich) was added immediately after irradiation to block S-G2 progression. After incubation, the cells were trypsinized, washed with PBS, and permeabilized with 0.2% Triton X-100 in PBS for 10 min at 4°C. Cells were then treated with 1x perm/wash buffer (0.5% Tween 20 and 0.5% bovine serum albumin in PBS), centrifuged, and fixed with 3% PFA and 2% sucrose in PBS for 15 min at room temperature. After washing with 1x perm/wash buffer, cells were incubated with anti-RPA antibody (Merck) in 1x perm/wash buffer at 37°C. After further washing with 1x perm/wash buffer, cells were incubated with an AlexFlor488-conjugated secondary antibody for 45 min in 1x perm/wash buffer at 37°C. After final washes, cells were resuspended in propidium iodide (Sigma-Aldrich) and 100 μg/mL RNase A (RBC) and analyzed using a Becton Dickinson FACSVerse flow cytometer with BD FACSuite software. G2 cells were identified based on their DNA content as assessed by propidium iodide staining. Data analysis was performed with FlowJo software.

Results

DDR proteins are present in nuclease – and high salt-resistant protein fraction

It has been suggested that several DSBR proteins are associated with the nuclear matrix (Mladenov et al. 2006, Xia et al. 2006). In a previous subcellular

fractionation study, we reported that replication proteins were present in nuclease – and high salt-resistant protein fractions, suggesting an association with stationary structures such as the nuclear matrix (Park et al. 2021). Based on these observations, we hypothesized that DDR proteins may also function while being associated with the nuclear matrix. To test this hypothesis, we extracted proteins from HEK293 T cells in a sequential manner (Figure 1A). We employed a nonionic detergent-based cell lysis method to meticulously isolate distinct protein fractions without disrupting their interactions (He et al. 1990). The first step involved lysing the cells with detergent to obtain the soluble fraction (Sol). The pellet was then digested with nuclease and eluted to yield the chromatin fraction (Ch). Following this, the pellet was washed with a high salt solution, after which it was solubilized with 8 M urea to obtain the nuclear matrix proteins and proteins associated with nuclease – and high salt-resistant chromatin (pellet fraction, Pe). The soluble, chromatin, and pellet fractions could be clearly distinguished based on the presence of α-tubulin, histone H3, and lamin proteins, respectively (Figure 1B).

We then examined the fractionation profile of DDR proteins (Figure 1C). The ATM protein was predominantly present in the soluble and pellet fractions. The MRN complex proteins were present in all three fractions, although the fractional abundance of each protein varied. MDC1 and RNF8, which are crucial for histone ubiquitination in the vicinity of DSB sites (Smeenk and Mailand 2016), exhibited distinct profiles. MDC1 was present in both the chromatin and pellet fractions, whereas RNF8 was only present in the latter. Furthermore, our findings indicate that BRAC1, RAP80, CtIP, 53BP1, and RIF1, which regulate DSB end resection and determine the DSBR pathway between HR and NHEJ, were predominantly present in the pellet fraction. As previously reported (Xia et al. 2006), BRCA2 was present in the pellet fraction. However, KU80, an NHEJ factor, was present in the soluble and chromatin fractions but not in the pellet fraction. The results suggest that the majority of DDR and DSBR proteins are associated with stationary structures. Furthermore, the latter has a significantly higher tendency for this association.

DDR proteins remain associated with stationary structures, regardless of DNA damage or cell cycle progression.

Previous studies identified an augmented association of DNA repair proteins, including RAD51, XRCC1, and PARP1, with the nuclear matrix in the context of DNA damage, such as X-ray irradiation or H_2O_2 treatment (Mladenov et al. 2006, Kubota et al. 2009). Given the presence of DDR and DSBR proteins in the pellet fraction, we sought to investigate the fractionation profile of these proteins upon DSB induction, with a particular focus on changes in the ATM and MRN complexes. Following ionizing radiation (IR) treatment, γH2AX and phosphorylation of two DNA damage checkpoint proteins, CHK1 at serine 345 (S345) and CHK2 at threonine 68 (T68), was increased, confirming the proper induction of DNA damage (Figure 1D). In the context of this condition, the fractionation profile of ATM and MRN complex proteins was not significantly affected by IR treatment, with the exception of a slight increase in the levels of ATM and MRN complex proteins and a significant increase in phosphorylation of ATM at S1981 [pATM (S1981)] in the pellet fraction at the recovery time point (Figure 1D), which suggests an increase in the association of ATM and MRN complex with the nuclear matrix. The level of RAD51 in the pellet fraction exhibited a gradual increase during the recovery period, in accordance with a previous report (Mladenov et al. 2006). Additionally, an increase in CtIP level in the pellet fraction was observed at all recovery time points.

We then proceeded to investigate the fraction profile of the ATM and MRN complex proteins in different cell cycle phases. We synchronized the cells at the G1/S boundary using a CDK1 inhibitor and thymidine block method, and released them from the block to obtain cells in each cell cycle phase (Figures 1E). As is well known, the level of PCNA in the chromatin fraction is high in the S phase, and histone H3 phosphorylation at serine 10 is only detected in G2/M phase (Figure 1F). We found that the fraction profile of ATM and MRN complex, as well as that of MDC1, was not significantly influenced by cell cycle phases, with the exception of a reduction in the levels of ATM in the pellet fraction in the S phase. On the other hand, the levels of RAD51 and CtIP in the pellet fractions were found to be significantly elevated in the S phase. When considered in conjunction with data obtained following DSB induction, these data suggest that initial DSB sensors, including the ATM and MRN complexes, stably associate with stationary structures throughout the cell cycle. This association persists even after the generation of DSBs, suggesting its role in efficient DNA damage sensing and repair of damaged DNA. Conversely, DSBR proteins, such as CtIP and RAD51, appear to increase their association with immobile structures tangled with damaged DNA when necessary.

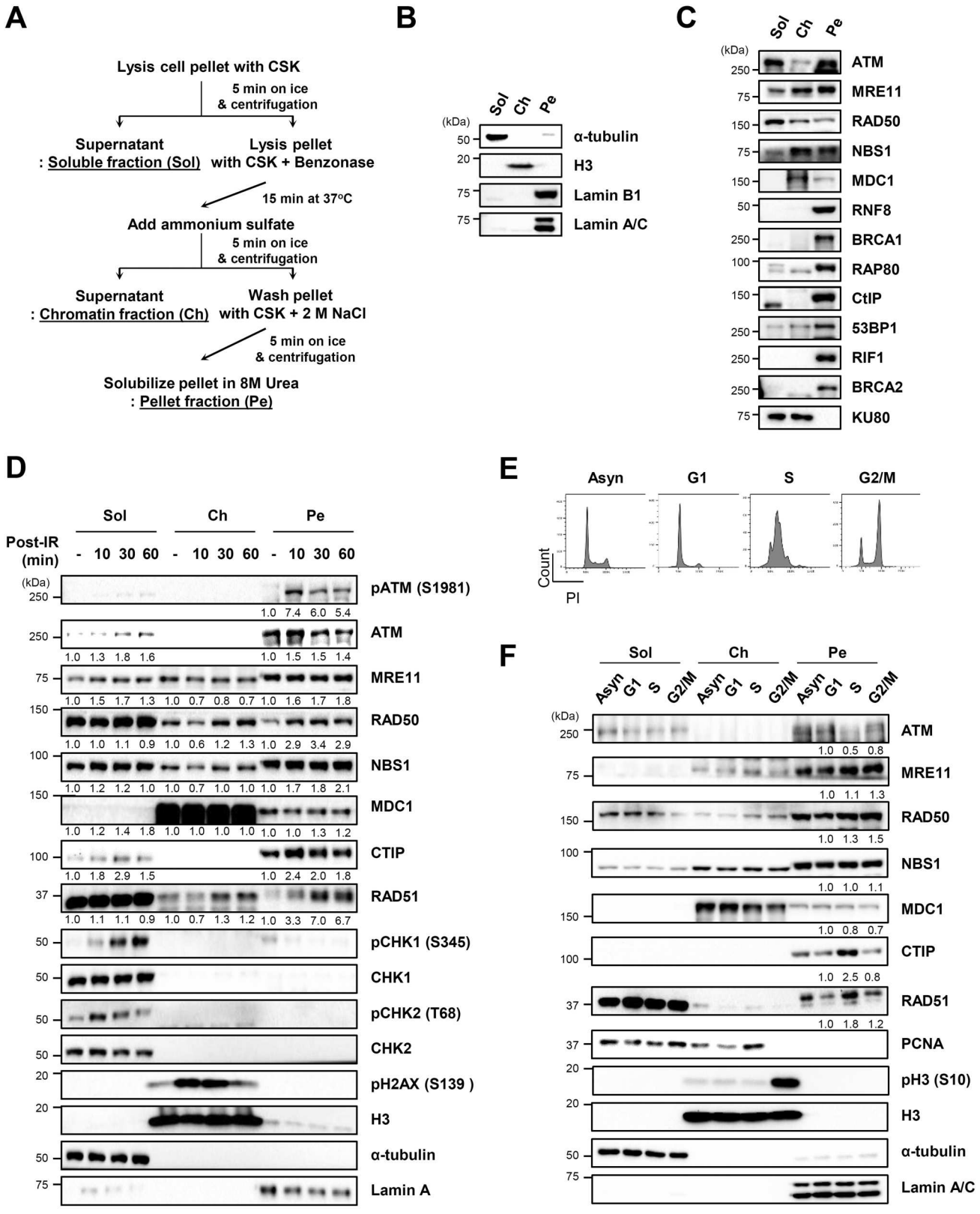

Figure 1. DDR proteins are present in nuclease – and high salt-resistant protein fraction throughout the cell cycle. (A) The scheme for protein fractionation method. Detailed procedure was described in the method section. (B-E, F) HEK293 T cells were fractionated as the scheme in (A). Soluble (Sol), chromatin (Ch), and pellet fraction (Pe) fractions were subjected to immunoblotting as indicated. (D) Cells were irradiated with 10 gray (Gy) X-ray and recovered for indicated times. The number below each band represents the relative band intensity divided by that of Lamin A and then normalized to the non-irradiated sample. (E, F) Cells were first arrested at G2 phase using CDK1 inhibitor (RO-3306) and released in media containing thymidine to arrest cells at G1/S boundary. Cells were then released into fresh media and incubated for 3 h (S), 8 h (G2/M) and 13 h (G1). Cells at each phase and asynchronous (Asyn) were fixed for propidium iodide (PI) staining (E) or fractionated for immunoblotting (F). (E) DNA content was measured by flow cytometry. (F) The number below each band represents the relative band intensity divided by that of Lamin A and then normalized to the G1 sample.

Lamin A/C interacts with ATM, MRE11 and RAD50

Structural proteins Lamin A/C and B are fundamental components of the nuclear lamina. In addition, nucleoplasmic Lamin A/C has long been postulated to compose a frame of the nuclear matrix. Previously, it was reported that Lamin A/C interacts with a DDR protein, 53BP1, which maintains the positional stability of DNA damage repair foci and regulates HR efficiency (Redwood et al. 2011, Mahen et al. 2013, Gibbs-Seymour et al. 2015). Consequently, we postulated that Lamin A/C serves as a structural platform for DDR proteins, including ATM and the MRN complex, to bind and accumulate in a highly efficient manner to sense damaged DNA. To test this hypothesis, we investigated the interaction of Lamin A/C with ATM, MRE11, and RAD50. Our findings revealed that immunoprecipitation of either green fluorescent protein (GFP)-fused Lamin A or GFP-fused Lamin C led to the pull-down of ATM, MRE11, and RAD50 (Figure 2A and B). Moreover, this interaction was not affected by IR treatment.

Lamin A/C enhances the association of ATM with the nuclear matrix during the DDR

We then examined the effects of Lamin A/C depletion on the levels of ATM and MRN complex proteins in the pellet fraction with or without IR treatment (Figure 3A). When Lamin A/C was depleted in IR-untreated cells using small interfering RNA (siRNA), the levels of ATM and MRN complex proteins in the pellet fraction were not reduced. Instead, those of RAD50 and NBS1 in the pellet fraction slightly increased. This pattern was consistently shown for MRN complex proteins even after IR treatment. However, the elevated levels of ATM and pATM (S1981) in the pellet fraction upon IR treatment were diminished following Lamin A/C depletion (Figure 3A). The results suggest that Lamin A/C may be involved in the increased association of ATM with the nuclear matrix following the DSB generation. The results also indicate that Lamin A/C plays a role in the initial DDR process, whereby it anchors ATM to the nuclear matrix through protein-protein interaction. Consistently, the levels of CtIP and RAD51 increased in the pellet fraction upon IR treatment were decreased when Lamin A/C was depleted. It is noteworthy that the combined levels of MDC1, CtIP, and RAD51 in all fractions were reduced in Lamin A/C-depleted cells, even in the absence of IR treatment (Figure 3A). This suggests the existence of an additional regulatory mechanism governing DDR/DSBR by Lamin A/C.

Lamin A/C facilitates the ATM-mediated DDR signals

The reduction in pATM (S1981) resulting from Lamin A/C depletion prompted us to investigate the impact on downstream DDR signals following ATM activation. We found that Lamin A/C depletion significantly impaired the phosphorylation of CHK1 at S345 and CHK2 at T68, as well as the phosphorylation of H2AX (γH2AX) in response to IR (Figure 3B). This data is consistent with a previous report indicating a reduction in H2AX phosphorylation in Hutchinson-Gilford progeria syndrome patient cells where the *LMNA* gene is mutated. (Zhang et al. 2016). Furthermore, the phosphorylation of NBS1 at S343 and P53 at S15, which is mediated by ATM kinase in the S-phase checkpoint pathway during the DDR (Lavin et al. 2015), was reduced when Lamin A/C was depleted (Figure 3C). The reduction in P53 phosphorylation at S15 upon Lamin A/C depletion may be a consequence of a general reduction in the protein level of P53, which was, in part, explained by a reduction in *P53* mRNA expression (Figure 3D).

Next, we investigated the effect of Lamin A/C depletion on ATM-mediated DDR signals, employing a precisely targeted DSB induction system based on FokI endonuclease. In this system, a cell expresses a fusion protein comprising FokI and FokI fused with mCherry fluorescence protein-Lac repressor (LacR). Upon tamoxifen treatment, the fusion protein enters the nucleus and binds to an array of lac operators pre-inserted in the genome via the Lac repressor, leading to FokI-mediated DSB generation (Shanbhag et al. 2010). Following the DSB induction, detergent-soluble and chromatin-bound proteins were removed using the same method employed for the immunoblot analysis, and the remaining pATM (S1981) were examined at the DSB sites (Figure 3E). The results demonstrated a reduction in pATM (S1981) upon Lamin A/C depletion (Figure 3E and F). The data collectively indicate that Lamin A/C is a critical for regulating ATM-mediated DDR signals.

Lamin A/C facilitates a constant interaction between ATM and MRN proteins

The phosphorylation of ATM at S1981 at the damaged site is partly regulated by its interaction with the MRN complex (Shiloh 2014). Defects in the phosphorylation of ATM at S1981 and its downstream DDR signals in Lamin A/C-depleted cells led us to investigate the interaction between ATM and the MRN complex. As previously reported (Shiloh 2014), FLAG-tagged ATM was shown to interact with MRE11 and RAD50 (Figure 4A). This interaction was reduced by Lamin A/C depletion,

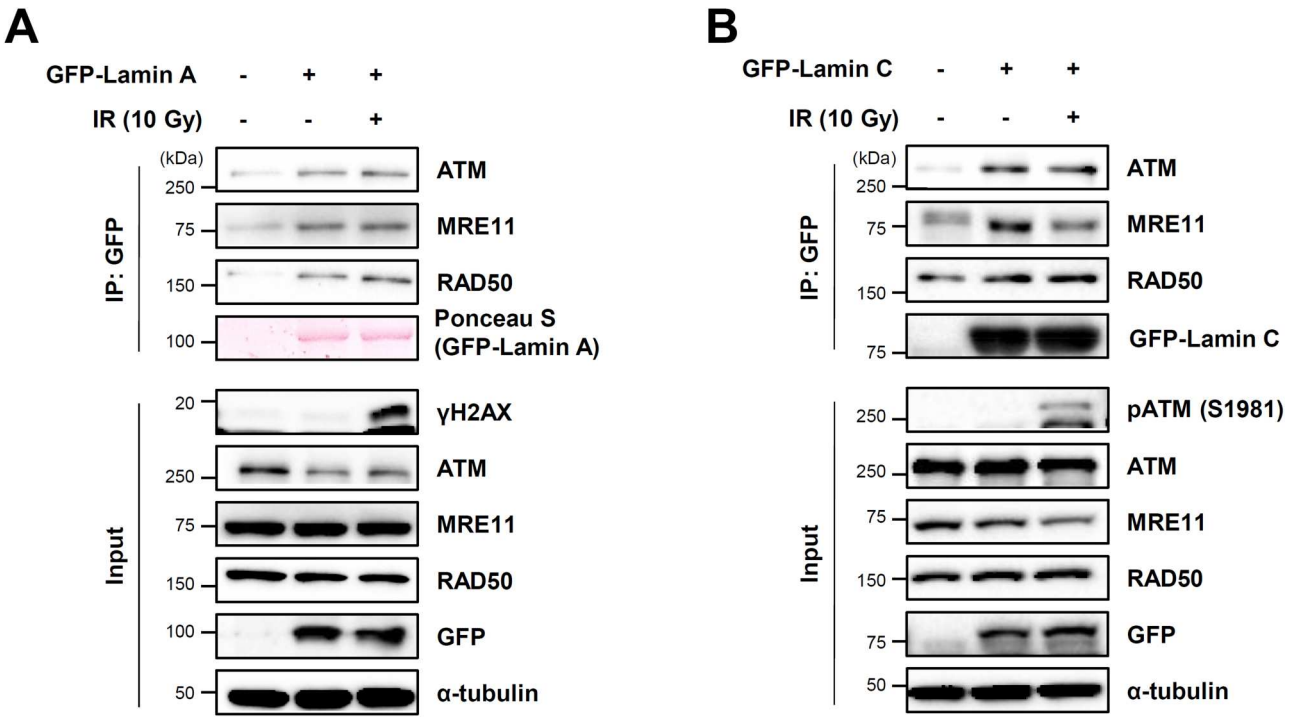

Figure 2. Lamin A/C interact with ATM, MRE11, and RAD50. (A, B) HEK293 T cells were transfected with control GFP vector or GFP-tagged Lamin A cDNA (A) or Lamin C cDNA (B). Forty-eight hours after transfection, cells were irradiated with 10 Gy X-ray and recovered for 30 min. Whole-cell extracts were immunoprecipitated with anti-GFP antibody followed by immunoblotting.

regardless of whether IR treatment was applied. These findings suggest that Lamin A/C may facilitate the interaction between ATM and the MRN complex.

Lamin A/C ensures efficient recruitment of MRE11 to the damaged DNA

The interaction between ATM and MRN represents one of the earliest DNA damage responses, which allows for the further recruitment of the MRN complex to the damaged DNA. Given that this interaction was hindered by Lamin A/C depletion, we examined the recruitment of MRE11 to the damaged DNA. Firstly, following the DSB induction at lac operators in the genome by FokI-LacR, MRE11 signals at the DSB sites were diminished in the Lamin A/C-depleted cells (Figure 4B and C), after detergent-soluble and chromatin-bound proteins were removed. This was also demonstrated when 355-nanometer ultraviolet (UV) microirradiation was applied, which revealed a reduction in MRE11 signals on the microirradiated strip (Figure 4D and E).

Previous reports have suggested that damaged DNA subjected to UV irradiation is tethered to the nuclear matrix (McCready and Cook 1984, Harless and Hewitt 1987, Koehler and Hanawalt 1996). Additionally, nuclear matrix-associated DNA is preferentially repaired (Mullenders et al. 1988). Consequently, we investigated the effect of Lamin A/C depletion on the association of damaged DNA with the nuclear matrix. The induction of DNA damage was achieved through the 355-nanometre UV microirradiation, with subsequent visualization of the DNA conducted through the application of DAPI staining (Figure 4F). The extraction of detergent-soluble and chromatin-bound fractions resulted in the removal of the majority of the DNA, as evidenced by a reduction in the overall DAPI signal. However, fragments of DNA that were bound to the nucleolus or nuclear envelope were resistant to nuclease and high-salt wash. As anticipated, the DAPI signal along the microirradiated strip was most prominent, indicating that damaged DNA is predominantly resistant to the nuclease and high-salt condition. We found that the DNA remaining on the microirradiated strip was significantly diminished, particularly when Lamin A/C was depleted (Figure 4F and G). In conjunction with a reduction in MRE11 at DNA damage sites following Lamin A/C depletion, these results suggest that the sustained association of the damaged DNA and DDR proteins with the nuclear matrix is facilitated by Lamin A/C.

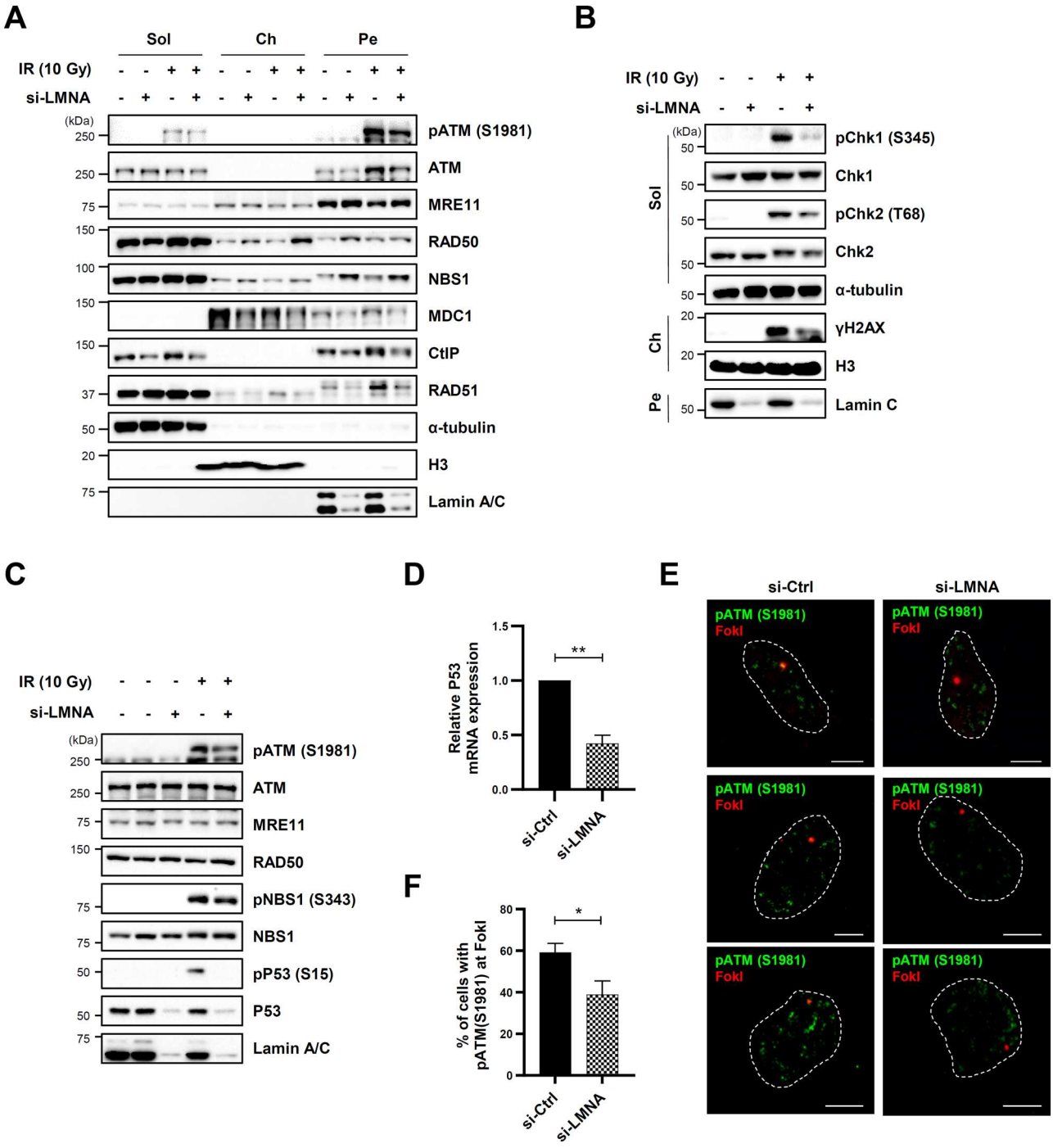

Figure 3. Lamin A/C depletion impedes the ATM-mediated DDR signals. (A-D) HEK293 T cells were transfected with *LMNA* siRNA. Forty-eight hours after transfection, cells were irradiated with 10 Gy X-ray and recovered for 30 min. Cells were fractionated (A, B) or whole-cell extracts was prepared (C) for immunoblotting. (D) RNA was isolated for qPCR. Error bars represent SEM (n = 3). (E, F) U2OS-LacO reporter cells stably expressing DD-ER-FokI-mCherry-LacR cells were transfected with *LMNA* siRNA, and after 48 h, DSB was induced by treatment with tamoxifen. Cells were fractionated, fixed, and stained for pATM (S1981). (E) Representative images. (F) Quantification of colocalization between pATM (S1981) and FokI. Scale bar, 5 μm. Error bars represent SEM (n = 3). (D, F) Statistical analysis: two-tailed unpaired student's t-test, $^*P < 0.05$.

Lamin A/C facilitates HR by maintaining transcript levels of CtIP and RAD51

DDR signals modulate downstream DSBR processes depending on the cell cycle and the availability of proteins responsible for each DSBR pathway. Since Lamin A/C depletion impairs DDR signaling, we examined the effects of Lamin A/C depletion on HR and NHEJ, the two main DSBR pathways, using I-*Sce*I-based

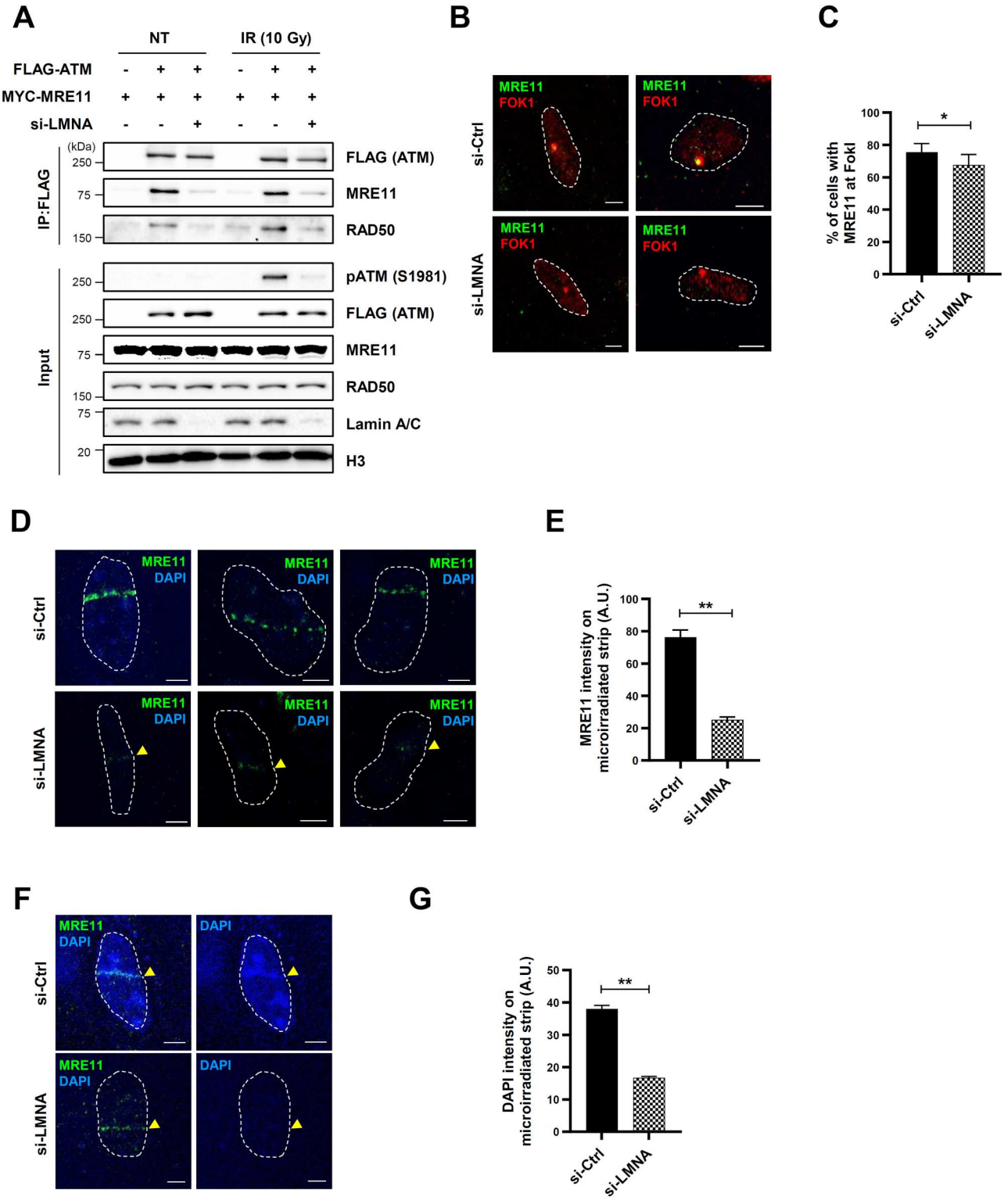

Figure 4. Lamin A/C depletion reduces the interaction between ATM and MRE11 (A) HEK293 T cells were co-transfected with Flag-ATM and Myc-MRE11 and either control or *LMNA* siRNA. Forty-eight hours after transfection, cells were irradiated with 10 Gy X-ray and recovered for 30 min. Whole-cell extracts were immunoprecipitated with anti-FLAG antibody followed by immunoblotting. (B, C) U2OS-LacO reporter cells stably expressing DD-ER-FokI-mCherry-LacR cells were transfected with *LMNA* siRNA, and after 48 h, DSB was induced by treatment with tamoxifen. Cells were fractionated, fixed, and stained for MRE11. (B) Representative images. (C) Quantification of colocalization between MRE11 and FokI. Error bars represent SEM (n = 6). (D-G) U2OS cells were transfected with *LMNA* siRNA for 48 h, UV-microirradiated, fractionated, fixed, and stained for MRE11. (D, F) Representative images. (E, G) Quantification of MRE11 signal intensity (E) or DAPI signal intensity (G) on microirradiated strips. Error bars represent SEM (n = 3). Scale bar, 5 μm. (A, C, E, G) Statistical analysis: two-tailed unpaired student's t-test, $^{**}P < 0.005$, $^{*}P < 0.05$.

reporter assays, scoring for the restoration of GFP expression (Gunn and Stark 2012). Lamin A/C depletion reduced the frequency of HR (Figure 5A), as reported (Redwood et al. 2011) while NHEJ remained intact (Figure 5B). Depletion of RAD51 and LIG4, which play key roles in HR and NHEH, reduced the frequency of HR and NHEJ, respectively (Figure 5A and B),

The observation of HR-specific defects following Lamin A/C depletion prompted us to investigate the modulation of proteins in HR in Lamin A/C-depleted cells. Given that the combined levels of CtIP and RAD51, the two principal HR factors, were reduced in all fractions following Lamin A/C depletion (Figure 3A), we wanted to confirm this result with the whole cell extracts. Consequently, the total protein levels of CtIP and RAD51, as well as MDC1, were reduced upon Lamin A/C depletion, while those of ATM and MRN proteins were not affected (Figure 5C).

To determine whether the reduction in protein levels of CtIP, RAD51, and MDC1 is mediated by a proteasome-dependent degradation pathway, cells were treated with a proteasome inhibitor, MG132, while new protein synthesis was blocked by the simultaneous treatment of cycloheximide. In control cells, cycloheximide treatment resulted in a reduction in the protein levels of CtIP and RAD51, which was restored by MG132 treatment (Figure 5C). This result suggests that CtIP and RAD51 undergo rapid protein turnover via a proteasomal degradation pathway. In Lamin A/C-depleted cells, the reduced protein level of CtIP was partially restored by MG-132 treatment, whereas the levels of RAD51 and MDC1 remained unaltered (Figure 5C). This suggests that a reduction in the protein levels of CtIP, RAD51, and MDC1 may result from other main regulatory processes in Lamin A/C-depleted cells. Consequently, we found that mRNA transcript levels of *CtIP, RAD51,* and *MDC1* were significantly reduced in Lamin A/C-depleted cells (Figure 5D), which suggests that Lamin A/C plays a regulatory role in the transcription of CtIP and RAD51.

CtIP is a resection enzyme that carries out DNA end resection, a critical step of HR (Sartori et al. 2007). In accordance with the reduction in CtIP protein level following Lamin A/C depletion, the recruitment of GFP-fused CtIP to the UV microirradiated strips was diminished in Lamin A/C-depleted cells (Figure 5E). Replication protein A 2 (RPA2) binds to the single-strand DNA exposed after DNA end resection. Flow cytometry analysis was employed to measure the loading of replication protein A 2 (RPA2) on resected DNA in G2 cells after IR treatment. The results showed that the intensity of RPA2 was reduced by CtIP depletion, as previously reported (Sartori et al. 2007), and moderately by Lamin A/C depletion as well (Figure 5F). Collectively, the data indicate that Lamin A/C plays a role in maintaining the level of HR factors, which is crucial for the efficacy of HR repair.

Discussion

In this report, we identified the subcellular localization of DDR proteins. Our findings indicate that a significant portion of DDR proteins associated with the nuclease – and high salt-resistant stationary structures, which are postulated to consist of nuclear matrix and nuclease-resistant chromatin. In particular, some DDR proteins, including ATM, RNF8, and BRCA2, were not observed to associate with nuclease-sensitive chromatin (Figure 1C). The high abundance of MRN complex proteins and MDC1 in chromatin fractions, in contrast to ATM, may be related to their association with actively transcribed regions for scanning transcription-associated DNA damage and initiating repair (Salifou et al. 2021). The overall fractionation profile of ATM and MRN was not significantly altered in response to the DSB induced by IR treatment (Figure 1D). However, the increase in the level of RAD51 and CtIP in the pellet fraction following IR treatment was observed with different kinetics. This indicates that proteins involved in the initial stages of the DDR, such as DSB sensors or mediators, may maintain an association with the nuclear matrix. This association may facilitate the efficient sensing of DNA damage and the subsequent relay of initial DDR signals to effector proteins. Accordingly, DSBR proteins such as CtIP and RAD51 appear to actively associate with the nuclear matrix and adjacent damaged DNA when necessary.

While the level of ATM in the pellet fraction exhibited a transient increase following DSB formation, the level of MRN proteins in the pellet fraction was not affected (Figure 1D). Previous reports have indicated that damaged DNA is tethered to the nuclear structure for efficient repair (McCready and Cook 1984, Harless and Hewitt 1987, Koehler and Hanawalt 1996, Belin et al. 2015). Additionally, our observations revealed an association between damaged DNA and the nuclear matrix (Figure 4F). Therefore, it can be assumed that the increase in the association of the MRN complex with the damaged DNA tethered to the nuclear matrix was not visible in the protein fractionation method due to its already high association with the nuclear matrix. In accordance with the aforementioned assumption, when DSBs were induced at specific sites of genomic DNA and detergent-soluble and chromatin-bound proteins were removed, MRE11 signals were observed at the DSB sites, similar to that observed for pATM (S1981).

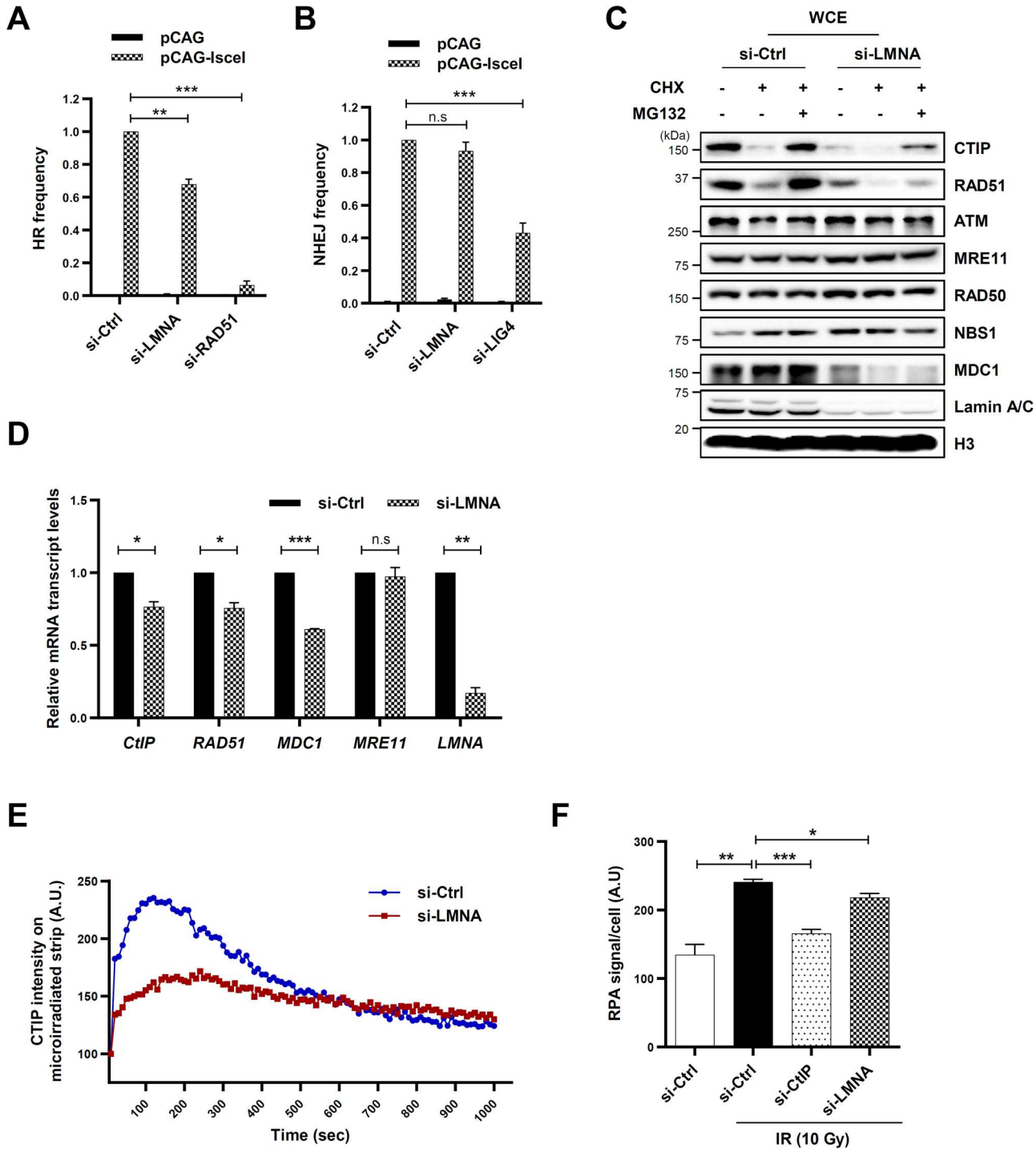

Figure 5. Lamin A depletion reduces the transcript levels of CtIP and RAD51 (A, B) DSBR frequency was measured 48 h after transfection with the I-SceI endonuclease using U2OS reporter cells transfected with *LMNA*, *RAD51*, or *LIG4* siRNA. Error bars represent SEM (n = 3). (C) HEK293 T cells transfected with *LMNA* siRNA were incubated with 10 mM cyclohexamide (CHX) or 10 μM MG132 for 12 h. Whole-cell extracts was prepared for immunoblotting. (D) HEK293 T cells were transfected with siRNA as indicated, and after 48 h, RNA was isolated for qPCR. Error bars represent SEM (n = 3). (E) HeLa cells were co-transfected with GFP-CtIP cDNA and either control or *LMNA* siRNA, and after 48 h, cells were subjected to UV microirradiation. Relative intensities, adjusted to the baseline of 100 are displayed. (F) HEK293 T cells transfected with *LMNA* or *CtIP* siRNA were subjected to mock treatment or X-ray (10 Gy), incubated for 2 h, and chromatin-bound RPA was detected in G2 cells by flow cytometry. Numbers in the graph indicate geometric mean. Error bars represent SEM (n = 3). (A, B, D, F) Statistical analysis: two-tailed unpaired student's t-test, ***$P < 0.0005$, **$P < 0.005$, *$P < 0.05$.

In Lamin A/C-depleted cells, the elevated levels of ATM and pATM (S1981) in the pellet fraction upon IR treatment, as well as pATM (S1981) and MRE11 signals at the DSB sites, were found to be diminished (Figures 3 and 4). Our findings indicate that Lamin A/C interacts with ATM and MRN complex proteins (Figure 2). However, this does not appear to be the regulatory mechanism underlying the augmented association of ATM and MRN with the nuclear matrix, as the interaction remained unchanged upon DSB. The interaction between the ATM and MRN complexes is essential for the initial activation of ATM as well as for the recruitment of further ATM molecules and the amplification of the ATM-mediated DNA damage response (DDR) signal (Shiloh 2014, Lavin et al. 2015). The results of our investigation indicate that the interaction between the ATM and MRN complexes was diminished in the context of Lamin A/C depletion (Figure 4A). We postulate that this might explain the reduced pATM (S1981) and MRE11 signals at the DSB sites and subsequent defects in checkpoint activation. The interaction of Lamin A/C with the ATM and MRN complex proteins may result in an increased probability of an interaction between the ATM and MRN complex. It has been reported that nuclear matrix-associated DNA is preferentially repaired (Mullenders et al. 1988). Therefore, it is also possible that the tethering of damaged DNA to the nuclear matrix may be regulated by Lamin A/C, as shown by the reduced level of damaged DNA at DSB sites in Lamin A/C-depleted cells (Figure 4G), which can increase the probability of an interaction between the ATM and MRN complex. Further studies are required to elucidate the precise mechanisms by which Lamin A/C regulates the interaction between the ATM and MRN complex, thereby facilitating efficient DDR signaling.

Our findings indicate that the frequency of HR is reduced in Lamin A/C-depleted cells (Figure 5A and B). This reduction in HR following Lamin A/C depletion has also been previously reported (Redwood et al., 2011b). The observed reduction in HR may be attributed to defects in ATM-mediated DDR signals resulting from Lamin A/C depletion, as we have demonstrated. Furthermore, we observed a reduction in mRNA transcript levels of a DDR protein, MDC1, and critical HR proteins, RAD51 and CtIP, in Lamin A/C-depleted cells (Figure 5D), which may be another contributing factor to HR defects. Lamin A/C has previously been reported to regulate the transcription of *RAD51* (Redwood, Perkins, et al. 2011). Additionally, it has been reported that Lamin A/C depletion results in the degradation of pRb and p107, which, in conjunction with E2F4, enhances *RAD51* mRNA transcription (Redwood, Gonzalez-Suarez, et al. 2011, Mayca Pozo et al. 2017). It remains to be determined whether MDC1 and CtIP are regulated in a similar manner by Lamin A/C. In conclusion, Lamin A/C plays a critical role in HR regulation by facilitating the initial ATM-mediated DDR signals and maintaining the level of HR proteins.

Mutations in the *LMNA* gene are associated with several degenerative diseases collectively known as laminopathies (Worman and Bonne 2007). In addition, alterations in A-type lamins have been associated with physiological aging, most notably in Hutchinson-Gilford Progeria Syndrome (HGPS), where a mutant prelamin A isoform called progerin is expressed (Liu et al. 2011). Although the exact etiology of diseases caused by to *LMNA* mutations remains unclear, DNA damage and genomic instability are being investigated as potential causes. Inflammation may be triggered when the pattern recognition receptors of innate immune cells mistake self-DNA for foreign DNA (Roers et al. 2016). Since *LMNA* deficiency is associated with genomic instability and premature aging (Liu et al. 2005, Graziano et al. 2018), self-DNA leaking into the cytoplasm due to genomic instability may activate innate immune responses and contribute to tumorigenesis and aging. Accordingly, HGPS cell and mouse models were reported to exhibit inflammatory markers, particularly an elevated NF-kB profile, which is associated with ATM activation (Osorio et al. 2012, Rouhi et al. 2022). A recent paper showed that high extracellular stiffness combined with Lamin A deficiency leads to nuclear rupture, causing mislocalization of DNA repair factors and consequent DNA damage (Cho et al. 2019), suggesting multiple pathways for the involvement of genomic instability in the etiology of LMNA mutations.

Our studies and others have shown that Lamin A/C regulates DDR signaling. However, there are also studies suggesting the opposite regulatory process. Regulation of Lamin A/C by the ATM and ATR has been reported to be critical for maintaining nuclear envelope (NE) integrity. A recent study shows that the inhibition or deletion of ATM reduces *LMNA* expression, resulting in increased nuclear deformability and enhanced cell migration through confined spaces due to substantial nuclear deformation (Shah et al. 2022). ATR has been reported to control chromosome integrity and chromatin dynamics, responding to mechanical stress by associating with the NE (Kumar et al. 2014).This modulation of NE plasticity and chromatin association by ATR activity is independent of DDR signaling. However, ATR plays a role in NE rupture upon DNA damage. ATR-dependent phosphorylation of Lamin A/C leads to changes in lamina assembly that cause NE rupture, particularly in cancer cells with DNA repair defects (Kovacs et al. 2023). Furthermore, the

involvement of ATR in embryonic stem cell differentiation under mechanical stress highlights its role in modulating Lamin A/C expression and nuclear compaction-mediated DDR (Roy et al. 2024). These findings underscore the critical functions of ATM and ATR in regulating Lamin A/C, thereby preserving NE integrity and facilitating cellular adaptation to mechanical and genotoxic stress.

In this report, we demonstrate that Lamin A/C is essential for the proper functioning of the DDR by facilitating the stable interaction between ATM and the MRN complex, which is critical for ATM activation and subsequent DDR signaling. We also show that Lamin A/C plays a critical role in ensuring efficient DSB resection and HR. Our research provides important insights into the mechanisms by which Lamin A/C modulates DDR and HR pathways, with potential implications for understanding the cellular responses to DNA damage and the maintenance of genomic integrity.

Disclosure statement

No potential conflict of interest was reported by the author(s).

Funding

This work was supported by the Institute for Basic Science (IBS-R022-D1) and Hallym University Research Fund (HRF-202304-003).

References

Aebi U, Cohn J, Buhle L, Gerace L. 1986. The nuclear lamina is a meshwork of intermediate-type filaments. Nature. 323:560–564. doi:10.1038/323560a0.

Bakkenist CJ, Kastan MB. 2003. DNA damage activates ATM through intermolecular autophosphorylation and dimer dissociation. Nature. 421:499–506. doi:10.1038/nature01368.

Belin BJ, Lee T, Mullins RD. 2015. DNA damage induces nuclear actin filament assembly by Formin -2 and Spire-(1/2) that promotes efficient DNA repair. Elife. 4:e07735.

Bridger JM, Kill IR, O'Farrell M, Hutchison CJ. 1993. Internal lamin structures within G1 nuclei of human dermal fibroblasts. J Cell Sci. 104(Pt 2):297–306. doi:10.1242/jcs.104.2.297.

Cho S, Vashisth M, Abbas A, Majkut S, Vogel K, Xia Y, Ivanovska IL, Irianto J, Tewari M, Zhu K, Tichy ED. 2019. Mechanosensing by the lamina protects against nuclear rupture, DNA damage, and cell-cycle arrest. Dev Cell. 49:920–935 e925. doi:10.1016/j.devcel.2019.04.020.

D'Amours D, Jackson SP. 2002. The Mre11 complex: at the crossroads of DNA repair and checkpoint signalling. Nat Rev Mol Cell Biol. 3:317–327. doi:10.1038/nrm805.

Dupre A, Boyer-Chatenet L, Gautier J. 2006. Two-step activation of ATM by DNA and the Mre11-Rad50-Nbs1 complex. Nat Struct Mol Biol. 13:451–457. doi:10.1038/nsmb1090.

Fontana GA, Reinert JK, Thoma NH, Rass U. 2018. Shepherding DNA ends: Rif1 protects telomeres and chromosome breaks. Microb Cell. 5:327–343. doi:10.15698/mic2018.07.639.

Gesson K, Rescheneder P, Skoruppa MP, von Haeseler A, Dechat T, Foisner R. 2016. A-type lamins bind both hetero- and euchromatin, the latter being regulated by lamina-associated polypeptide 2 alpha. Genome Res. 26:462–473. doi:10.1101/gr.196220.115.

Gibbs-Seymour I, Markiewicz E, Bekker-Jensen S, Mailand N, Hutchison CJ. 2015. Lamin A/C-dependent interaction with 53BP1 promotes cellular responses to DNA damage. Aging Cell. 14:162–169. doi:10.1111/acel.12258.

Gonzalez-Suarez I, Redwood AB, Perkins SM, Vermolen B, Lichtensztejin D, Grotsky DA, Morgado-Palacin L, Gapud EJ, Sleckman BP, Sullivan T, Sage J. 2009. Novel roles for A-type lamins in telomere biology and the DNA damage response pathway. EMBO J. 28:2414–2427. doi:10.1038/emboj.2009.196.

Graziano S, Kreienkamp R, Coll-Bonfill N, Gonzalo S. 2018. Causes and consequences of genomic instability in laminopathies: replication stress and interferon response. Nucleus. 9:258–275.

Groelly FJ, Fawkes M, Dagg RA, Blackford AN, Tarsounas M. 2023. Targeting DNA damage response pathways in cancer. Nat Rev Cancer. 23:78–94. doi:10.1038/s41568-022-00535-5.

Guelen L, Pagie L, Brasset E, Meuleman W, Faza MB, Talhout W, Eussen BH, De Klein A, Wessels L, De Laat W, Van Steensel B. 2008. Domain organization of human chromosomes revealed by mapping of nuclear lamina interactions. Nature. 453:948–951. doi:10.1038/nature06947.

Gunn A, Stark JM. 2012. I-SceI-based assays to examine distinct repair outcomes of mammalian chromosomal double strand breaks. Methods Mol Biol. 920:379-391.

Harless J, Hewitt RR. 1987. Intranuclear localization of UV-induced DNA repair in human VA13 cells. Mutat Res. 183:177–184.

He DC, Nickerson JA, Penman S. 1990. Core filaments of the nuclear matrix. J Cell Biol. 110:569–580. doi:10.1083/jcb.110.3.569.

Kijas AW, Lim YC, Bolderson E, Cerosaletti K, Gatei M, Jakob B, Tobias F, Taucher-Scholz G, Gueven N, Oakley G, Concannon P. 2015. ATM-dependent phosphorylation of MRE11 controls extent of resection during homology directed repair by signalling through Exonuclease 1. Nucleic Acids Res. 43:8352–8367. doi:10.1093/nar/gkv754.

Kind J, Pagie L, Ortabozkoyun H, Boyle S, de Vries SS, Janssen H, Amendola M, Nolen LD, Bickmore WA, van Steensel B. 2013. Single-cell dynamics of genome-nuclear lamina interactions. Cell. 153:178–192. doi:10.1016/j.cell.2013.02.028.

Kind J, van Steensel B. 2014. Stochastic genome-nuclear lamina interactions: modulating roles of Lamin A and BAF. Nucleus. 5:124–130. doi:10.4161/nucl.28825.

Koehler DR, Hanawalt PC. 1996. Recruitment of damaged DNA to the nuclear matrix in hamster cells following ultraviolet irradiation. Nucleic Acids Res. 24:2877–2884. doi:10.1093/nar/24.15.2877.

Kovacs MT, Vallette M, Wiertsema P, Dingli F, Loew D, Nader GPF, Piel M, Ceccaldi R. 2023. DNA damage induces nuclear envelope rupture through ATR-mediated phosphorylation of Lamin A/C. Mol Cell. 83:3659–3668 e3610. doi:10.1016/j.molcel.2023.09.023.

Kubota Y, Takanami T, Higashitani A, Horiuchi S. 2009. Localization of X-ray cross complementing gene 1 protein in the nuclear matrix is controlled by casein kinase II-dependent phosphorylation in response to oxidative damage. DNA Repair (Amst). 8:953–960. doi:10.1016/j.dnarep.2009.06.003.

Kumar A, Mazzanti M, Mistrik M, Kosar M, Beznoussenko GV, Mironov AA, Garre M, Parazzoli D, Shivashankar GV, Scita G, Bartek J. 2014. ATR mediates a checkpoint at the nuclear envelope in response to mechanical stress. Cell. 158:633–646. doi:10.1016/j.cell.2014.05.046.

Lavin MF, Kozlov S, Gatei M, Kijas AW. 2015. ATM-dependent phosphorylation of all three members of the MRN complex: from sensor to adaptor. Biomolecules. 5:2877–2902. doi:10.3390/biom5042877.

Lee JH, Paull TT. 2005. ATM activation by DNA double-strand breaks through the Mre11-Rad50-Nbs1 complex. Science. 308:551–554.

Lee KY, Park SH. 2020. Eukaryotic clamp loaders and unloaders in the maintenance of genome stability. Exp Mol Med. 52:1948–1958. doi:10.1038/s12276-020-00533-3.

Lee SJ, Jung YS, Yoon MH, Kang SM, Oh AY, Lee JH, Jun SY, Woo TG, Chun HY, Kim SK, Chung KJ. 2016. Interruption of progerin-lamin A/C binding ameliorates Hutchinson-Gilford progeria syndrome phenotype. J Clin Invest. 126:3879–3893. doi:10.1172/JCI84164.

Li BX, Chen J, Chao B, Zheng Y, Xiao X. 2018. A lamin-binding ligand inhibits homologous recombination repair of DNA double-strand breaks. ACS Cent Sci. 4:1201–1210.

Liu B, Wang J, Chan KM, Tjia WM, Deng W, Guan X, Huang JD, Li KM, Chau PY, Chen DJ, Pei D. 2005. Genomic instability in laminopathy-based premature aging. Nat Med. 11:780–785. doi:10.1038/nm1266.

Liu GH, Barkho BZ, Ruiz S, Diep D, Qu J, Yang SL, Panopoulos AD, Suzuki K, Kurian L, Walsh C, Thompson J. 2011. Recapitulation of premature ageing with iPSCs from Hutchinson-Gilford progeria syndrome. Nature. 472:221–225. doi:10.1038/nature09879.

Mahen R, Hattori H, Lee M, Sharma P, Jeyasekharan AD, Venkitaraman AR. 2013. A-type lamins maintain the positional stability of DNA damage repair foci in mammalian nuclei. PLoS One. 8:e61893.

Mayca Pozo F, Tang J, Bonk KW, Keri RA, Yao X, Zhang Y. 2017. Regulatory cross-talk determines the cellular levels of 53BP1 protein, a critical factor in DNA repair. J Biol Chem. 292:5992–6003. doi:10.1074/jbc.M116.760645.

McCready SJ, Cook PR. 1984. Lesions induced in DNA by ultraviolet light are repaired at the nuclear cage. J Cell Sci. 70:189–196. doi:10.1242/jcs.70.1.189.

Mladenov E, Anachkova B, Tsaneva I. 2006. Sub-nuclear localization of Rad51 in response to DNA damage. Genes Cells. 11:513–524. doi:10.1111/j.1365-2443.2006.00958.x.

Moir RD, Spann TP, Herrmann H, Goldman RD. 2000. Disruption of nuclear lamin organization blocks the elongation phase of DNA replication. J Cell Biol. 149:1179–1192. doi:10.1083/jcb.149.6.1179.

Moir RD, Yoon M, Khuon S, Goldman RD. 2000. Nuclear lamins A and B1: different pathways of assembly during nuclear envelope formation in living cells. J Cell Biol. 151:1155–1168. doi:10.1083/jcb.151.6.1155.

Mullenders LH, van Kesteren van Leeuwen AC, van Zeeland AA, Natarajan AT. 1988. Nuclear matrix associated DNA is preferentially repaired in normal human fibroblasts, exposed to a low dose of ultraviolet light but not in Cockayne's syndrome fibroblasts. Nucleic Acids Res. 16:10607–10622. doi:10.1093/nar/16.22.10607.

Osorio FG, Barcena C, Soria-Valles C, Ramsay AJ, de Carlos F, Cobo J, Fueyo A, Freije JM, Lopez-Otin C. 2012. Nuclear lamina defects cause ATM-dependent NF-kappaB activation and link accelerated aging to a systemic inflammatory response. Genes Dev. 26:2311–2324. doi:10.1101/gad.197954.112.

Park SH, Kim SJ, Myung K, Lee KY. 2021. Characterization of subcellular localization of eukaryotic clamp loader/unloader and its regulatory mechanism. Sci Rep. 11:21817. doi:10.1038/s41598-021-01336-w.

Qiao F, Moss A, Kupfer GM. 2001. Fanconi anemia proteins localize to chromatin and the nuclear matrix in a DNA damage- and cell cycle-regulated manner. J Biol Chem. 276:23391–23396. doi:10.1074/jbc.M101855200.

Redwood AB, Gonzalez-Suarez I, Gonzalo S. 2011. Regulating the levels of key factors in cell cycle and DNA repair: new pathways revealed by Lamins. Cell Cycle. 10:3652–3657. doi:10.4161/cc.10.21.18201.

Redwood AB, Perkins SM, Vanderwaal RP, Feng Z, Biehl KJ, Gonzalez-Suarez I, Morgado-Palacin L, Shi W, Sage J, Roti-Roti JL, Stewart CL. 2011. A dual role for A-type lamins in DNA double-strand break repair. Cell Cycle. 10:2549–2560. doi:10.4161/cc.10.15.16531.

Roers A, Hiller B, Hornung V. 2016. Recognition of endogenous nucleic acids by the innate immune system. Immunity. 44:739–754. doi:10.1016/j.immuni.2016.04.002.

Rogakou EP, Pilch DR, Orr AH, Ivanova VS, Bonner WM. 1998. DNA double-stranded breaks induce histone H2AX phosphorylation on serine 139. J Biol Chem. 273:5858–5868. doi:10.1074/jbc.273.10.5858.

Rouhi L, Auguste G, Zhou Q, Lombardi R, Olcum M, Pourebrahim K, Cheedipudi SM, Asghar S, Hong K, Robertson MJ, Coarfa C. 2022. Deletion of the Lmna gene in fibroblasts causes senescence-associated dilated cardiomyopathy by activating the double-stranded DNA damage response and induction of senescence-associated secretory phenotype. J Cardiovasc Aging. 2. doi:10.20517/jca.2022.14.

Roy T, Piplani N, Sthanam LK, Ghosh S, Tiwary N, Dhar S, Konyak WCW, Panigrahi SS, Singh P, Sowpati DT, Nair S. 2024. Nuclear compression-mediated DNA damage drives ATR-dependent Lamin expression and mouse ESC differentiation. bioRxiv. 2024–03. doi:10.1101/2024.03.15.585216.

Salifou K, Burnard C, Basavarajaiah P, Grasso G, Helsmoortel M, Mac V, Depierre D, Franckhauser C, Beyne E, Contreras X, Dejardin J. 2021. Chromatin-associated MRN complex protects highly transcribing genes from genomic instability. Sci Adv. 7. doi:10.1126/sciadv.abb2947.

Sartori AA, Lukas C, Coates J, Mistrik M, Fu S, Bartek J, Baer R, Lukas J, Jackson SP. 2007. Human CtIP promotes DNA end resection. Nature. 450:509–514. doi:10.1038/nature06337.

Savic V, Yin B, Maas NL, Bredemeyer AL, Carpenter AC, Helmink BA, Yang-Iott KS, Sleckman BP, Bassing CH. 2009. Formation of dynamic gamma-H2AX domains along broken DNA strands is distinctly regulated by ATM and MDC1 and dependent upon H2AX densities in chromatin. Mol Cell. 34:298–310. doi:10.1016/j.molcel.2009.04.012.

Shah P, McGuigan CW, Cheng S, Vanpouille-Box C, Demaria S, Weiss RS, Lammerding J. 2022. ATM modulates nuclear

mechanics by regulating Lamin A levels. Front Cell Dev Biol. 10: 875132.

Shanbhag NM, Rafalska-Metcalf IU, Balane-Bolivar C, Janicki SM, Greenberg RA. 2010. ATM-dependent chromatin changes silence transcription in cis to DNA double-strand breaks. Cell. 141:970–981. doi:10.1016/j.cell.2010.04.038.

Shibata A. 2017. Regulation of repair pathway choice at two-ended DNA double-strand breaks. Mutat Res. 803-805:51–55.

Shibata A, Conrad S, Birraux J, Geuting V, Barton O, Ismail A, Kakarougkas A, Meek K, Taucher-Scholz G, Löbrich M, Jeggo PA. 2011. Factors determining DNA double-strand break repair pathway choice in G2 phase. EMBO J. 30:1079–1092. doi:10.1038/emboj.2011.27.

Shiloh Y. 2006. The ATM-mediated DNA-damage response: taking shape. Trends Biochem Sci. 402–410. doi:10.1016/j.tibs.2006.05.004.

Shiloh Y. 2014. ATM: expanding roles as a chief guardian of genome stability. Exp Cell Res. 329:154–161. doi:10.1016/j.yexcr.2014.09.002.

Shimi T, Pfleghaar K, Kojima SI, Pack CG, Solovei I, Goldman AE, Adam SA, Shumaker DK, Kinjo M, Cremer T, Goldman RD, et al. 2008. The A- and B-type nuclear Lamin networks: microdomains involved in chromatin organization and transcription. Genes Dev. 22:3409–3421. doi:10.1101/gad.1735208.

Smeenk G, Mailand N. 2016. Writers, readers, and erasers of histone ubiquitylation in DNA double-strand break repair. Front Genet. 7:122.

Spann TP, Moir RD, Goldman AE, Stick R, Goldman RD. 1997. Disruption of nuclear lamin organization alters the distribution of replication factors and inhibits DNA synthesis. J Cell Biol. 136:1201–1212. doi:10.1083/jcb.136.6.1201.

Stucki M, Clapperton JA, Mohammad D, Yaffe MB, Smerdon SJ, Jackson SP. 2005. MDC1 directly binds phosphorylated histone H2AX to regulate cellular responses to DNA double-strand breaks. Cell. 123:1213–1226. doi:10.1016/j.cell.2005.09.038.

van Steensel B, Belmont AS. 2017. Lamina-associated domains: links with chromosome architecture, heterochromatin, and gene repression. Cell. 169:780–791. doi:10.1016/j.cell.2017.04.022.

Worman HJ, Bonne G. 2007. "Laminopathies": a wide spectrum of human diseases. Exp Cell Res. 313:2121–2133. doi:10.1016/j.yexcr.2007.03.028.

Xia B, Sheng Q, Nakanishi K, Ohashi A, Wu J, Christ N, Liu X, Jasin M, Couch FJ, Livingston DM. 2006. Control of BRCA2 cellular and clinical functions by a nuclear partner, PALB2. Mol Cell. 22:719–729. doi:10.1016/j.molcel.2006.05.022.

Zhang H, Sun L, Wang K, Wu D, Trappio M, Witting C, Cao K. 2016. Loss of H3K9me3 correlates with ATM activation and histone H2AX phosphorylation deficiencies in Hutchinson-Gilford progeria syndrome. PLoS One. 11:e0167454.